ISSN: 0067-2904

The Peristaltic Flow of Williamson Fluid through a Flexible Channel

Dheia G. Salih Al-Khafajy*, Walaa N. Al-Delfi
Department of Mathematics, College of Science, University of Al-Qadisiyah, Diwaneyah, *Iraq*

Received: 28/2/2022 Accepted: 1/8/2022 Published: 28/2/2023

Abstract

The purpose of this study is to investigate the effect of an elastic wall on the peristaltic flow of Williamson fluid between two concentric cylinders, where the inner tube is cylindrical with an inelastic wall and the outer wall is a regular elastic sine wave. For this problem, cylindrical coordinates are used with a short wavelength relative to channel width for its length, as well as the governing equations of Williamson fluid in the Navier-Stokes equations. The results evaluated using the Mathematica software program. The Mathematica program used by entering the various data for the parameters, where the program shows the graphs, then the effect of these parameters became clear and the results mentioned in the conclusion. Williamson fluid peristaltic flow through an elastic conduit is the subject of this investigation. For a number of significant elements, such as velocity distribution, stress and wave frame streamlines, graphic findings are supplied at the end of the article.

Keywords: Williamson fluid, peristaltic flow**,** wall properties**,** cylindrical coordinates**.**

التدفق التمعجي لمائع ويليامسون عبر قناة مرنة

ضياء غازي صالح الخفاجي* ، ولاء ناصر خضير الدلفي
قسم الرياضيات ، كلية العلوم ، جامعة القادسية ، الديوانية ، العراق

الخلاصة

الغرض من هذه الدراسة هو التحقق من تأثير الجدار المرن على التدفق التمعجي لسائل ويليامسون بين أسطوانتين متحدتين المركز ، حيث يكون الأنبوب الداخلي أسطوانيًا بجدار غير مرن والجدار الخارجي عبارة عن موجة جيبية مرنة منتظمة. لهذه المشكلة ، تم استخدام الإحداثيات الأسطوانية ، بالإضافة إلى الطول الموجي القصير بالنسبة لعرض القناة لطولها بالإضافة إلى المعادلات الحاكمة لسائل ويليامسون في معادلات نافيير–ستوكس ، وتم تقييم النتائج باستخدام برنامج **Mathematica**. تم استخدام برنامج **Mathematica** عن طريق إدخال البيانات المختلفة للمعلمات ، حيث أظهر البرنامج الرسوم البيانية ، ثم أصبح تأثير هذه المعلمات واضحًا وتم ذكر النتائج في الخاتمة. إن التدفق التمعجي لسائل ويليامسون عبر قناة مرنة هو موضوع هذا التحقيق. بالنسبة لعدد من العناصر المهمة ، مثل توزيع السرعة والإجهاد وتبسيط إطار الموجة ، يتم توفير النتائج الرسومية في نهاية المقالة.

*Email: dr.dheia.g.salih@gmail.com

1. Introduction

Predicated by the wave of area contraction and expansion that travels together with the distensible tube or channel, peristaltic flow occurs. Bolus formation, ureter flow, chyme advancement in the gastrointestinal system, embryo transport in the uterine cavity, and blood flow in arteries are all examples of peristalsis. For example, in the nuclear sector, researchers have used this mechanism to describe peristaltic and roller pumps, as well as the transportation of dangerous and destructive fluids and heart-lung machines. Numerous scholars have studied peristaltic transport in a varied configuration because of its widespread usage in a variety of scientific domains. Peristaltic transport of non-Newtonian fluid has been of paramount importance to researchers in bioengineering and medicine because of its wide range of applications in sectors such as biotechnology and physiology [1–6].

Latham's [7] initial investigation on peristalsis paved way for many scholars to study and analyze the peristaltic motion (Shapiro [8], Yin and Fung [9]). Tang and Fung [10] are among the numerous writers who have presented their research with the opinion that many physiological fluids, including blood, flow under peristalsis behave like a Newtonian fluid. Although he proposed Newtonian and non-Newtonian fluid models for physiological flow. Salman & Ali studied the combined effects of the porous medium and heat transfer on MHD Jeffery fluid which flows through a two dimensional asymmetric, inclined tapered channel [11], in his work they have results show a parabolic behavior, it rises in the central part of the channel and decreases due to the effect of Hartmann's number, while the opposite behavior appears through the effect of the porosity modulus. Almusawi and Abdulhadi presented and discussed a Ree–Eyring fluid's peristaltic transport in a rotating frame and examines the impacts of MHD [12].

The peristaltic flow of fluids through a rubber channel has an important role in the food and medical industries, in addition to the movement of blood in the arteries, food in the intestines and liquids in the human body. All this suggests the elasticity of the wall of the flow channel has an important role in the movement of fluids. Al-Khafajy and Abdulhadi studied the effects of wall properties and heat transfer on the peristaltic transport of Jeffrey, Carreau, and Williamson fluids through a porous medium channel in three different studies [13-15]. These and other studies were in Cartesian coordinates, this prompted us to study the peristaltic flow of Williamson's fluid between two concentric cylinders, an inner tube is cylindrical with an inelastic wall and an outer wall is a regular elastic sine wave in the cylindrical coordinates.

2. Mathematical Formulation

Consider the peristaltic flow of Williamson fluid through two concentric cylinders, the inside tube is cylindrical and the outside is a regular elastic wall in the shape of a sine wave. The cylindrical coordinates are represented by R along the radius of the tube and Z synchronously with the axis of the tube as in Figure 1. We know the geometry of the wall surface as follows;

Inner wall

$$\bar{r} = \bar{r_1} = a_1$$

Outer wall

$$\bar{r} = \bar{r_2}(\bar{z}, \bar{t}) = a_2 + b\, Sin\left(\frac{2\pi}{\mathcal{L}}(\bar{z} - s\bar{t})\right)$$

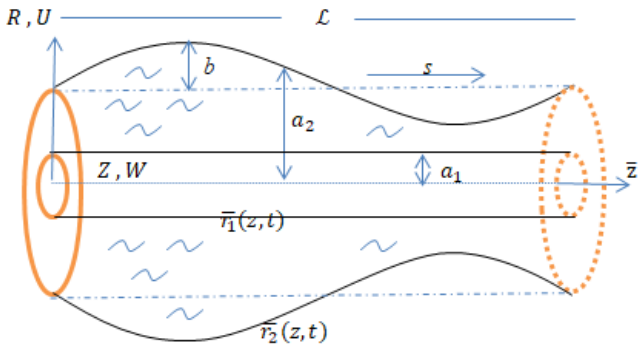

Figure 1: The problem Geometry

where a_2 is the average radius of the undisturbed tube, b is the amplitude of a peristaltic wave,$\mathcal{L}$ is a wavelength,s is a wave propagation speed, and $\bar{t}$ is a time.

3. Constitutive Equations

Basic equations governing continuity and the Navier-Stokes equations are

$$\nabla \bar{V} = 0 \tag{1}$$

$$\rho(\bar{V} \,.\, \bar{\nabla}\,)\bar{V} = \bar{\nabla}(-\bar{p}\,\bar{I} + \bar{\tau}) \tag{2}$$

Where $\bar{V}$ is the velocity field, ρ is density, $\bar{p}$ is pressure, $\bar{I}$ identity tensor, $\bar{\tau}$ is extra stress tensor and $\bar{\nabla}\bar{V}$ the fluid velocity gradient of Williamson's fluid is defined as:

$$\bar{\tau} = -[\mu_\infty + (\mu_0 + \mu_\infty)(1 - \Gamma\dot{\bar{\gamma}})^{-1}]\dot{\bar{\gamma}} \quad . \tag{3}$$

here μ_∞ is an infinite shear viscosity, μ_0 is a zero shear rate viscosity, Γ is the time constant and $\dot{\gamma}$ is shear strain.

Let $\bar{V}(v_1, v_2, v_3)$ be the velocity vector at cylindrical coordinates$(\mathrm{r}, \vartheta, \mathrm{z})$. The shear strain tensor is illustrated as follows:

$$\dot{\gamma} = 2E = \begin{bmatrix} 2\dfrac{\partial v_1}{\partial r} & \dfrac{1}{r}\left(\dfrac{\partial v_1}{\partial \vartheta} - v_2 + r\dfrac{\partial v_2}{\partial r}\right) & \dfrac{\partial v_1}{\partial z} + \dfrac{\partial v_3}{\partial r} \\ \dfrac{1}{r}\left(\dfrac{\partial v_2}{\partial \vartheta} - v_2 + r\dfrac{\partial v_2}{\partial r}\right) & \dfrac{2}{r}\left(\dfrac{\partial v_2}{\partial \vartheta} + v_1\right) & \dfrac{\partial v_2}{\partial z} + \dfrac{1}{r}\dfrac{\partial v_3}{\partial \vartheta} \\ \dfrac{\partial v_1}{\partial z} + \dfrac{\partial v_3}{\partial r} & \dfrac{\partial v_2}{\partial z} + \dfrac{1}{r}\dfrac{\partial v_3}{\partial \vartheta} & 2\dfrac{\partial v_3}{\partial z} \end{bmatrix}$$

4. Flexible wall

The equation governing the motion of an elastic wall can be expressed as $L^* = \bar{p} - \bar{p}_0$, where L^* is an operator, which is used to represent the motion of stretched membrane with viscosity damping forces such that

$$L^* = A\frac{\partial^4}{\partial \bar{Z}^4} - B\frac{\partial^2}{\partial \bar{Z}^2} + C\frac{\partial^2}{\partial \bar{t}^2} + D\frac{\partial}{\partial \bar{t}} + E_L$$

where A is a flexural rigidity of a wall, B is a longitudinal tension per unit width, C is a mass per unit area, D is a coefficient of viscous damping and E_L is a spring stiffness.
The governing equation for flexible wall canal properties at $\bar{r} = \bar{r_2}$ is found;

$$\frac{\partial \bar{\mathrm{P}}}{\partial \bar{z}} = \frac{\partial}{\partial \bar{\mathrm{Z}}}\left(A\frac{\partial^4}{\partial \bar{Z}^4} - B\frac{\partial^2}{\partial \bar{Z}^2} + C\frac{\partial^2}{\partial \bar{t}^2} + D\frac{\partial}{\partial \bar{t}} + E_L\right)(\bar{r_2}).$$

5. Solution Method

We write the speed components in an unstable two-dimensional flow as follows: $\overline{\mathrm{V}} = \left(\overline{V_1}(\bar{r},\bar{z},\bar{t}), 0, \overline{V_3}(\bar{r},\bar{z},\bar{t})\right)$, here $\overline{V_1}$ and $\overline{V_3}$ represent speed components corresponding to the radial and axial direction in a given frame, respectively.

The governing equations are got for fluid motion after replacing the velocity components in the shear stress equations for Williamson's fluid, then in Eq. (1) and Eq.(2), we have

$$\frac{\partial\overline{V_1}}{\partial\bar{R}} + \frac{\overline{V_1}}{\bar{R}} + \frac{\partial\overline{V_3}}{\partial\bar{Z}} = 0 \tag{4}$$

$$\rho\left(\frac{\partial\overline{V_1}}{\partial\bar{t}} + \overline{V_1}\frac{\partial\overline{V_1}}{\partial\bar{R}} + \overline{V_3}\frac{\partial\overline{V_1}}{\partial\bar{Z}}\right) = -\frac{\partial\bar{p}}{\partial\bar{R}} + \frac{1}{\bar{R}}\frac{\partial}{\partial\bar{R}}(\bar{R}\bar{\tau}_{\bar{R}\bar{R}}) + \frac{\partial}{\partial\bar{Z}}(\bar{\tau}_{\bar{R}\bar{Z}}) - \frac{\bar{\tau}_{\bar{\vartheta}\bar{\vartheta}}}{\bar{R}} \tag{5}$$

$$\rho\left(\frac{\partial\overline{V_3}}{\partial\bar{t}} + \overline{V_1}\frac{\partial\overline{V_3}}{\partial\bar{R}} + \overline{V_3}\frac{\partial\overline{V_3}}{\partial\bar{Z}}\right) = -\frac{\partial\bar{p}}{\partial\bar{Z}} + \frac{1}{\bar{R}}\frac{\partial}{\partial\bar{R}}(\bar{R}\bar{\tau}_{\bar{R}\bar{Z}}) + \frac{\partial}{\partial\bar{Z}}(\bar{\tau}_{\bar{Z}\bar{Z}}) \tag{6}$$

and the components of the extra stress are;

$$\bar{\tau}_{\bar{R}\,\bar{R}} = 2(\mu_0 + (\mu_0 - \mu_0)\Gamma\dot{\gamma})\left(2\frac{\partial\overline{V_1}}{\partial\bar{\mathrm{R}}}\right) \tag{7}$$

$$\bar{\tau}_{\bar{R}\,\bar{Z}} = (\mu_0 + (\mu_0 - \mu_\infty)\Gamma\dot{\gamma})\left(\frac{\partial\overline{V_1}}{\partial\bar{\mathrm{Z}}} + \frac{\partial\overline{V_3}}{\partial\bar{\mathrm{R}}}\right) \tag{8}$$

$$\bar{\tau}_{\bar{Z}\bar{Z}} = 2(\mu_0 + (\mu_0 - \mu_\infty)\Gamma\dot{\gamma})$$

The corresponding boundary conditions are:

$$\left.\begin{aligned} &\overline{V_3} = \overline{V_1} = 0\,, at\ \ \bar{r} = \overline{r_1} = a_1 \\ &\overline{V_3} = \overline{V_1} = 0\ \ , at\ \bar{r} = \overline{r_2}(\bar{z},\bar{t}) = a_2 + b\,Sin\left(\frac{2\pi}{\mathcal{L}}(\bar{z} - s\bar{t})\right) \end{aligned}\right\} \tag{10}$$

General and special two-frame coordinate transformations are given as follows;

$$\bar{r} = \bar{R}, \bar{z} = \bar{Z} - s\bar{t} \tag{11}$$

$$\overline{v_1} = \overline{V_1}, \overline{v_3} = \overline{V_3} - s \tag{12}$$

For $(\bar{r},\bar{z})$ and $(\overline{V_1},\overline{V_3})$ are also the components of velocity in the moving and static frames, respectively. By using these transforms, the equations the problem are:

$$\frac{\partial\overline{v_1}}{\partial\bar{r}} + \frac{\overline{v_1}}{\bar{r}} + \frac{\partial(\overline{v_3}+s)}{\partial\bar{z}} = 0 \tag{13}$$

$$\rho\left(\frac{\partial\overline{v_1}}{\partial\bar{t}} + \overline{v_1}\frac{\partial\overline{v_1}}{\partial\bar{r}} + (\overline{v_3}+s)\frac{\partial\overline{v_1}}{\partial\bar{z}}\right) = -\frac{\partial\bar{p}}{\partial\bar{r}} + \frac{1}{\bar{r}}\frac{\partial}{\partial\bar{r}}(\bar{r}\bar{\tau}_{\bar{r}\bar{r}}) + \frac{\partial}{\partial\bar{z}}(\bar{\tau}_{\bar{r}\bar{z}}) - \frac{\bar{\tau}_{\bar{\vartheta}\bar{\vartheta}}}{\bar{r}} \tag{14}$$

$$\rho\left(\frac{\partial(\overline{v_3}+s)}{\partial\bar{t}} + \overline{v_1}\frac{\partial(\overline{v_3}+s)}{\partial\bar{r}} + (\overline{v_3}+s)\frac{\partial(\overline{v_3}+s)}{\partial\bar{z}}\right) = -\frac{\partial\bar{p}}{\partial\bar{z}} + \frac{1}{\bar{r}}\frac{\partial}{\partial\bar{r}}(\bar{r}\bar{\tau}_{\bar{r}\bar{z}}) + \frac{\partial}{\partial\bar{z}}(\bar{\tau}_{\bar{z}\bar{z}}) \tag{15}$$

with the governing motion equation on the elastic wall, we get

$$\left(A\frac{\partial^5}{\partial\bar{z}^5} - B\frac{\partial^3}{\partial\bar{z}^3} + C\frac{\partial^3}{\partial\bar{z}\partial t^2} + D\frac{\partial^2}{\partial\bar{Z}^2} + E_l\frac{\partial}{\partial\bar{z}}\right)(\overline{r_2}) = \frac{1}{r}\frac{\partial}{\partial\bar{r}}(\bar{r}\bar{\tau}_{\bar{r}\bar{z}}) + \frac{\partial}{\partial\bar{z}}(\bar{\tau}_{\bar{z}\bar{z}}) - \rho\left(\frac{d(\overline{v_3}+s)}{\partial\bar{t}} + \overline{v_1}\frac{d(\overline{v_3}+s)}{\partial\bar{r}} + (\overline{v_3}+s)\frac{\partial(\overline{v_3}+s)}{\partial\bar{z}}\right) \tag{16}$$

In order to solve the equations controlling motion, we present non-dimensional equations to simplify these equations

$$\left.\begin{aligned} &v_1 = \frac{\overline{v_1}L}{a_2 s}, v_3 = \frac{\overline{v_3}}{s}, r = \frac{\bar{r}}{a_2}, z = \frac{\bar{z}}{L}, t = \frac{s\bar{t}}{L}, \tau = \frac{a_2\bar{\tau}}{s\mu_0}, \delta = \frac{a_2}{L}, W_e = \frac{\Gamma s}{a_2}, \dot{\gamma} = \frac{a_2\bar{\dot{\gamma}}}{s} \\ &p = \frac{a_2^2\bar{p}}{sL\mu_0}, Re = \frac{\rho s a_2}{\mu_0}, r_1 = \frac{\bar{r}_1}{a_2} = \varepsilon < 1, \emptyset = \frac{b}{a_2}, r_2 = \frac{\bar{r}_2}{a_2} = 1 + \emptyset\sin(2\pi\bar{z}) \end{aligned}\right\} \tag{17}$$

where $\emptyset$ the amplitude ratio, Re Reynolds number, δ the dimensionless wave number, and W_eWeissenberg number.

Substituting equation (17) into the components of the extra stress equations (7-9), equations (13-16), and the boundary conditions (10), respectively. We have

$$\left(\frac{S}{L}\right)\left(\frac{\partial v_1}{\partial r}+\frac{v_1}{r}+\frac{\partial v_3}{\partial z}\right)=0 \tag{18}$$

$$Re\delta^3\left(\frac{\partial v_1}{\partial t}+v_1\frac{\partial v_1}{\partial r}+(v_3+1)\frac{\partial v_1}{\partial z}\right)=-\frac{\partial p}{\partial r}+\delta\frac{1}{r}\frac{\partial}{\partial r}(r\tau_{rr})+\delta\frac{\partial}{\partial z}(\tau_{rz})-\delta\frac{\tau_{\theta\theta}}{r} \tag{19}$$

$$Re\delta\left(\frac{\partial v_3}{\partial t}+v_1\frac{\partial v_3}{\partial r}+(v_3+1)\frac{\partial v_3}{\partial z}\right)=-\frac{\partial p}{\partial z}+\frac{1}{r}\frac{\partial}{\partial r}(r\tau_{rz})+\delta\frac{\partial}{\partial z}\tau_{zz} \tag{20}$$

And the equation of motion governing the elastic wall

$$\left(\frac{Aa_2^3}{\mu sL^5}\right)\frac{\partial^5 r_2}{\partial z^5}-\left(\frac{Ba_2^3}{\mu sL^3}\right)\frac{\partial^3 r_2}{\partial z^3}+\left(\frac{Csa_2^3}{\mu L^3}\right)\frac{\partial^3 r_2}{\partial z\partial t^2}+\left(\frac{Da_2^3}{\mu L^2}\right)\frac{\partial^2 r_2}{\partial z\partial t}+\left(\frac{E_L a_2^3}{\mu sL}\right)\frac{\partial r_2}{\partial z}$$
$$=\frac{1}{r}\frac{\partial}{\partial r}(r\tau_{rz})+\delta\frac{\partial}{\partial z}\tau_{zz}-Re\delta\left(\frac{\partial v_3}{\partial t}+v_1\frac{\partial v_3}{\partial r}+(v_3+1)\frac{\partial v_3}{\partial z}\right) \tag{21}$$

where:

$$\bar{\tau}_{\bar{r}\bar{r}}=\ 2\mu_\circ(1+\Gamma|\bar{\dot{\gamma}}|)\left(2\frac{\partial\overline{v_1}}{\partial\bar{r}}\right)$$

$$\bar{\tau}_{\bar{r}\bar{z}}=\ \mu_\circ(1+\Gamma|\bar{\dot{\gamma}}|)\left(\frac{\partial\overline{v_1}}{\partial\bar{z}}+\frac{\partial\overline{v_3}}{\partial\bar{r}}\right)$$

$$\bar{\tau}_{\bar{z}\bar{z}}=\ 2\mu_\circ(1+\Gamma|\bar{\dot{\gamma}}|)\left(2\frac{\partial(\overline{v_3}+s)}{\partial\bar{z}}\right)$$

This gives boundary conditions with respect to dimensionless variables in the wave framework:

$$\left.\begin{aligned} &v_3=-1,\ v_1=0,\ at\ \ ra_2=\ r_1a_2=a_2a_1\\ &v_3=-1,\ v_1=0,\ at\ \ ra_2=\ r_2a_2(\bar{z},\bar{t})=a_2+b\,Sin\left(\frac{2\pi}{\mathcal{L}}(z\mathcal{L}-s\frac{\mathcal{L}t}{s})\right)\end{aligned}\right\} \tag{22}$$

6. Solutions of the Problem

It is very difficult to solve the problem in the latter form so we assume a very small wave-number ($\delta \ll 1$), hence equations (18-21) become:

$$\frac{\partial v_1}{\partial r}+\frac{v_1}{r}+\frac{\partial v_3}{\partial z}=0 \tag{23}$$

$$\frac{\partial p}{\partial r}=0 \tag{24}$$

$$\frac{\partial p}{\partial z}=\frac{1}{r}\frac{\partial}{\partial r}(r\tau_{rz}) \tag{25}$$

$$L_1\frac{\partial^5 r_2}{\partial z^5}+L_2\frac{\partial^3 r_2}{\partial z^3}+L_3\frac{\partial^3 r_2}{\partial z\partial t^2}+L_4\frac{\partial^2 r_2}{\partial z\partial t}+L_5\frac{\partial r_2}{\partial z}=\frac{1}{r}\frac{\partial}{\partial r}(r\tau_{rz}) \tag{26}$$

where $L_1=\frac{Aa_2^3}{\mu sL^5}$ is a flexural stiffness of the wall, $L_2=-\frac{Ba_2^3}{\mu sL^3}$ is a longitudinal tension per unit width, $L_3=\frac{Csa_2^3}{\mu L^3}$ is a mass per unit area, $L_4=\frac{Da_2^3}{\mu L^2}$ is a coefficient of viscid damping, and $L_5=\frac{E_La_2^3}{\mu sL}$ is spring stiffness is the spring stiffness. The components of the extra stress, are $\tau_{rr}=\tau_{zz}=0\ and\ \ \tau_{rz}=\left(\frac{\partial v_3}{\partial r}+We\left(\frac{\partial v_3}{\partial r}\right)^2\right)$.

Using the accepted assumption ($\delta \ll 1$), the components of the additional shear stress will be dimensionless as follow;

$$\tau_{rz}=\left(\frac{\partial v_3}{\partial r}+We\left(\frac{\partial v_3}{\partial r}\right)^2\right) \tag{27}$$

Replacing τ_{rz} into equation (26), we have;

$$r\frac{\partial^2 v_3}{\partial r^2}+\frac{\partial v_3}{\partial r}+We\left(\frac{\partial v_3}{\partial r}\right)^2+2rWe\left(\frac{\partial v_3}{\partial r}\right)\left(\frac{\partial^2 v_3}{\partial r^2}\right)=rK \tag{28}$$

with boundary conditions is $v_3(\varepsilon)=v_3(r_2)=-1$.

where $K = L_1 \frac{\partial^5 r_2}{\partial z^5} + L_2 \frac{\partial^3 r_2}{\partial z^3} + L_3 \frac{\partial^3 r_2}{\partial z \partial t^2} + L_4 \frac{\partial^2 r_2}{\partial z \partial t} + L_5 \frac{\partial r_2}{\partial z}$.
The corresponding stream function is $v_1 = -\frac{1}{r}\frac{\partial \psi}{\partial z}$ and $v_3 = \frac{1}{r}\frac{\partial \psi}{\partial r}$.

7. Perturbation Method Solution

In this section, we find the momentum function, shear stress function and stream function. The equation (28) is a nonlinear equation and the exact solution may not be possible, therefore, in order to find the solution, we employ the regular perturbation method in terms of a variant of We Weissenberg number for a second order. For perturbation solution, we expand as

$$v_3 = v_{03} + We v_{13} + We^2 v_{23} + O(We^3) \quad (29)$$

Substituting equation (29) into equation (28) with boundary conditions, then equating the like powers of We, we obtain

7.1. Zero order

$r \frac{\partial^2 v_{03}}{\partial r^2} + \frac{\partial v_{03}}{\partial r} = rK$
With boundary conditions $v_{03} = -1$ at $r = \varepsilon$ and $r = 1 + \emptyset . Sin\big(2\pi(z-t)\big)$.

7.2. First order

$r \frac{\partial^2 v_{13}}{\partial r^2} + \frac{\partial v_{13}}{\partial r} = -2\mathrm{r}\left(\frac{\partial^2 v_{03}}{\partial r^2}\right)\left(\frac{\partial v_{03}}{\partial r}\right) - \left(\frac{\partial v_{03}}{\partial r}\right)^2$
With boundary conditions $v_{13} = 0$ at $r = \varepsilon$ and $r = 1 + \emptyset . Sin\big(2\pi(z-t)\big)$.

7.3. Second order

$r \frac{\partial^2 v_{23}}{\partial r^2} + \frac{\partial v_{23}}{\partial r} = -2\mathrm{r}\left(\frac{\partial^2 v_{03}}{\partial r^2}\right)\left(\frac{\partial v_{13}}{\partial r}\right) - 2\mathrm{r}\left(\frac{\partial^2 v_{13}}{\partial r^2}\right)\left(\frac{\partial v_{03}}{\partial r}\right) - 2\left(\frac{\partial v_{03}}{\partial r}\right)\left(\frac{\partial v_{13}}{\partial r}\right)$

With boundary conditions $v_{23} = 0$ at $r = \varepsilon$ and $r = 1 + \emptyset . Sin\big(2\pi(z-t)\big)$.

The formula for the solutions obtained (velocity , shear stress, and stream function) is too long. The accompanying constants can be determined using the accompanying boundary conditions. Thus, we will discuss these solutions through graphs in the following section.

8. Discussion and Results

In this section, we discuss the results that we obtained after solving the equations of the problem using the perturbation method and then using a MATHEMATICA program to draw these results. This section has been divided into three parts: the first discusses the influence of parameters on the movement of the fluid through the flow channel, the second includes a discussion of the influence of parameters on shear stress and the last discusses the influence of parameters on the fluid flow paths.

8.1. Velocity profile

Figures 2-5 illustrate effect parameters W_e, $\emptyset$, L_1, L_2, L_3, L_4, L_5, and ε on the distribution of velocity v_3 vs. r, respectively. We notice in Figure 2 and 3 that the velocity is positively affected by the increase with parameters W_e, $\emptyset$, L_1 and L_2, respectively. Figure 4 shows that the velocity distribution decreases with the increasing of parameters L_3 and L_4, respectively. In Figure 5, observed that the velocity distribution rises with increasing parameter L_5 and falls down with increasing ε.

8.2. Shear Stress

In this section, we discuss the effect of parameters $\emptyset$, L_1, L_2, L_5, L_3, L_4, ε, and W_e on the shear stress, as we notice in Figures 6-9 that the stress increases on the solid wall (the inner wall of the channel) where its value is positive and in the middle of the channel the stress turns into a negative amount and its value decreases at the wall elastic (the outer wall of the channel) under the influence of the increase in the parameters $\emptyset$, L_1, L_2, and L_5, respectively. While in Figures 10 and 11,we notice the effect of parameters L_3 and L_4 opposite to the previous parameters as the stress decreases on the solid wall (the inner wall of the channel) where its value is positive and in the center of the channel, the stress turns into a negative amount and its value increases at the elastic wall (the outer wall of the channel). We note the effect of parameters ε and W_e on stress directly according to Figures 12, 13.

8.3. Phenomena Trapping

The closed streamlines of the bolus are formed thanks to the peristaltic motion of the wall of the flow channel affecting the fluid flow within the channel. in this section we will discuss the effect of parameters $\emptyset$, W_e, L_1, L_2, L_5, L_3, L_4, and ε on the trapped bolus.

Through Figures 14-18 we see that the trapped bolus increases and grows steadily in the center of the channel and expands to the outer wall (elastic wall) with increasing parameters $\emptyset$, W_e, L_1, L_2, and L_5, respectively, and vice versa for the parameters L_3, L_4, and ε where their effect is the contraction of the trapped bolus when these parameters are increased, respectively, in Figures 19-21.

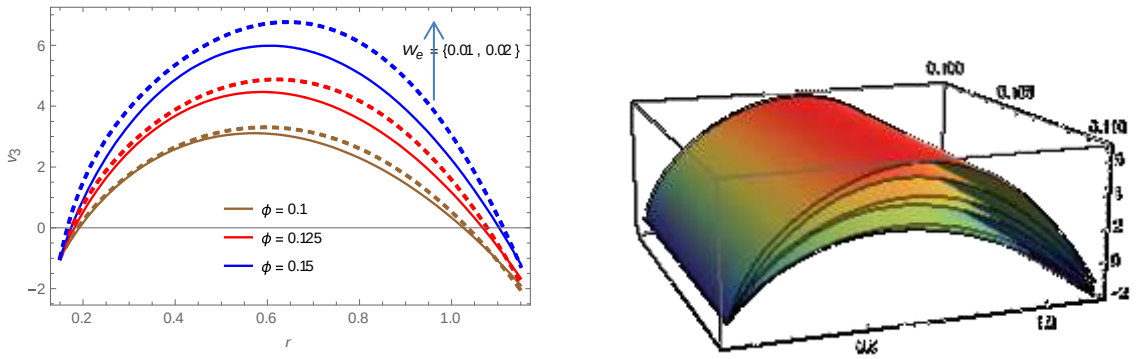

Figure 2: Velocity distribution for various values of W_e and $\emptyset$ with $\varepsilon = 0.15$, $L_1 = 0.1$, $L_2 = 0.5$, $L_3 = 0.1$, $L_4 = 0.1$, $L_5 = 0.1$, $t = 0.1$, $z = 0.4$.

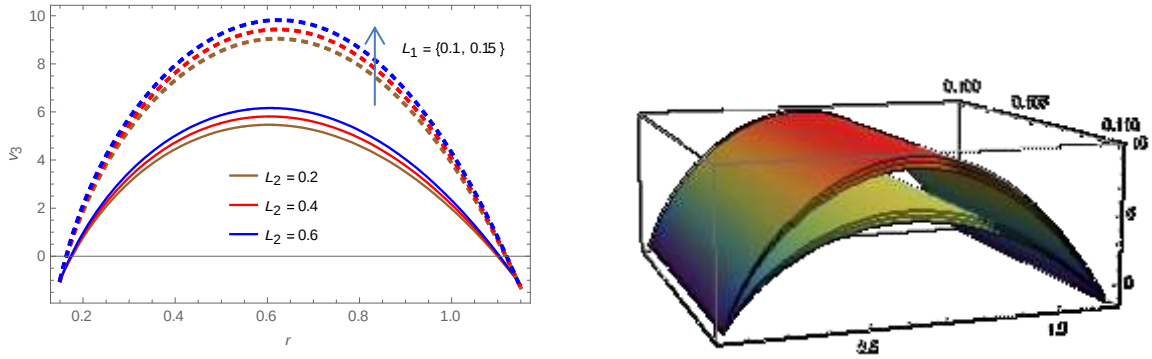

Figure 3: Velocity distribution for various values of L_1 and L_2 with $\emptyset = 0.15$, $\varepsilon = 0.15$, $W_e = 0.01$, $L_3 = 0.1$, $L_4 = 0.1$, $L_5 = 0.1$, $t = 0.1$, $z = 0.4$.

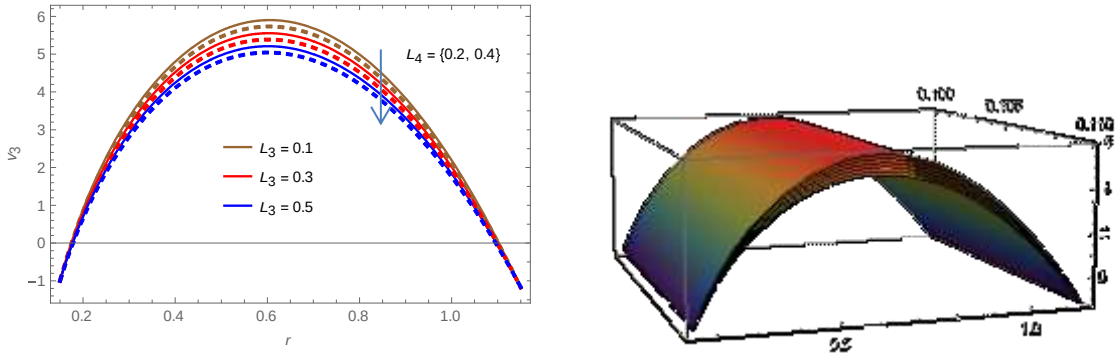

Figure 4: Velocity distribution for various values of L_3 and L_4 with $\emptyset = 0.15, \varepsilon = 0.15, W_e = 0.01, L_1 = 0.1, L_2 = 0.5, L_5 = 0.1, t = 0.1, z = 0.4$.

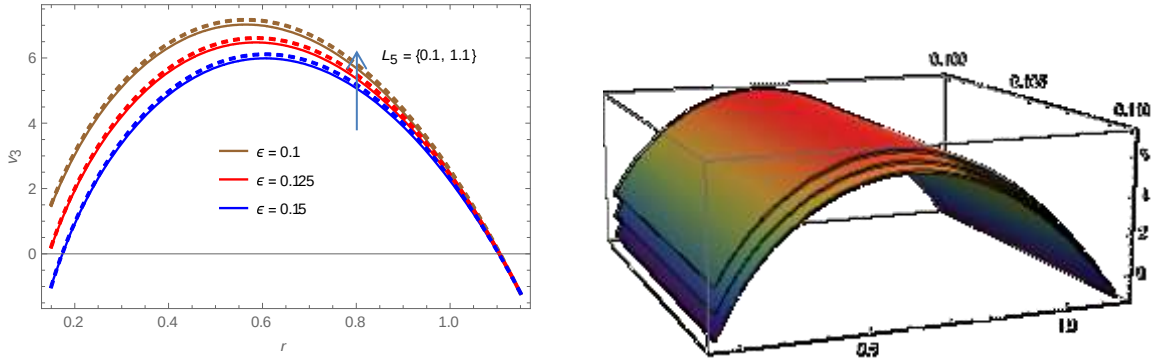

Figure 5 Velocity distribution for various values of L_5 and ε with $\emptyset = 0.15, W_e = 0.01, L_1 = 0.1, L_2 = 0.5, L_3 = 0.1, L_4 = 0.1, t = 0.1, z = 0.4$.

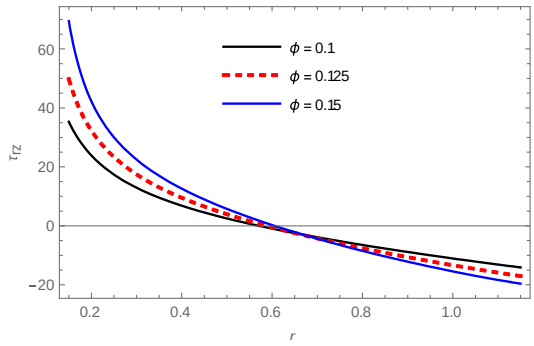

Figure 6 Shear-Stress for various values of $\emptyset$ with $\varepsilon = 0.15, t = 0.1, L_1 = 0.1, L_2 = 0.5, L_3 = 0.1, L_4 = 0.1, L_5 = 0.1, W_e = 0.01, z = 0.4$.

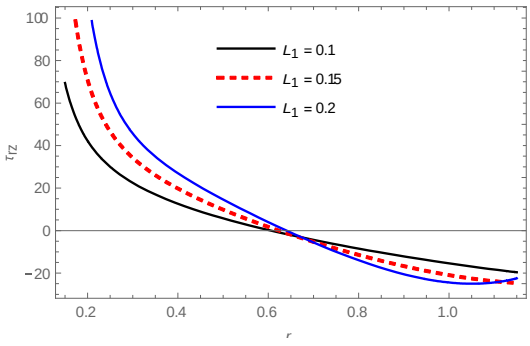

Figure 7 Shear-Stress for various values of L_1 with $\varepsilon = 0.15, t = 0.1, L_2 = 0.5, L_3 = 0.1, L_4 = 0.1, L_5 = 0.1, \emptyset = 0.15, W_e = 0.01, z = 0.4$.

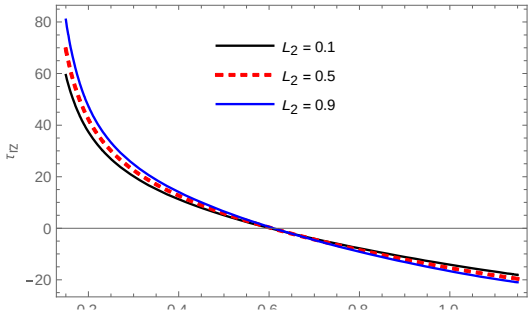

Figure 8 Shear-Stress for various values of L_2 with $\varepsilon = 0.15, t = 0.1, L_1 = 0.1, L_3 = 0.1, L_4 = 0.1, L_5 = 0.1, \emptyset = 0.15, W_e = 0.01, z = 0.4$.

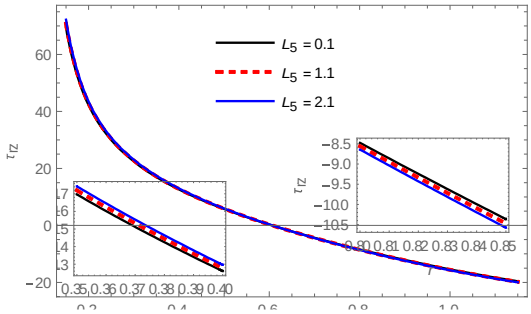

Figure 9 Shear-Stress for various values of L_5 with $\varepsilon = 0.15, t = 0.1, L_1 = 0.1, L_3 = 0.1, L_4 = 0.1, L_5 = 0.1, \emptyset = 0.15, W_e = 0.01, z = 0.4$.

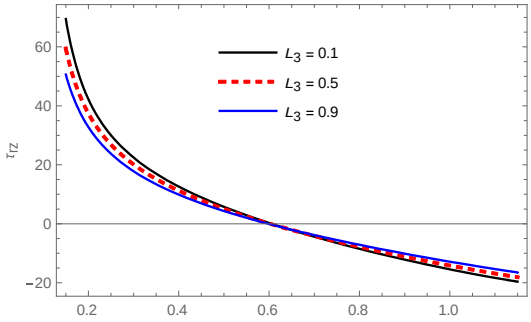

Figure 10 Shear-Stress for various values of L_3 with $\varepsilon = 0.15, t = 0.1, L_1 = 0.1, L_2 = 0.5, L_4 = 0.1, L_5 = 0.1, \emptyset = 0.15, W_e = 0.01, z = 0.4$.

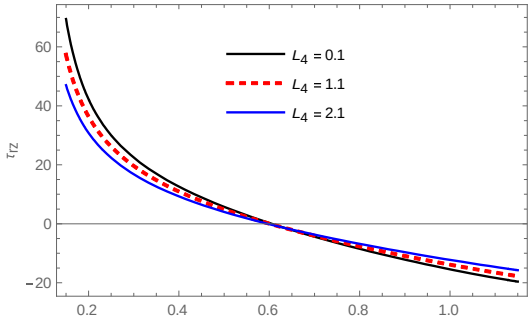

Figure 11 Shear-Stress for various values of L_4 with $\varepsilon = 0.15, t = 0.1, L_1 = 0.1, L_2 = 0.5, L_3 = 0.1, L_5 = 0.1, \emptyset = 0.15, W_e = 0.01, z = 0.4$.

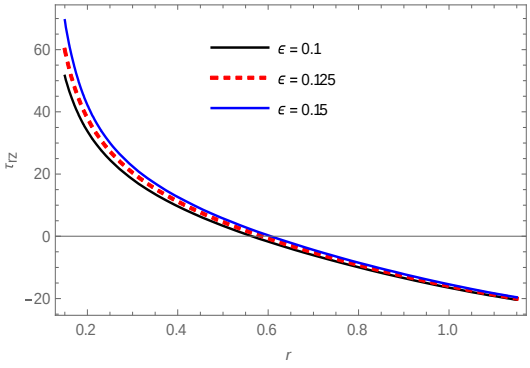

Figure 12 Shear-Stress for various values of ε with $\emptyset = 0.15, t = 0.1, L_1 = 0.1, L_2 = 0.5, L_3 = 0.1, L_4 = 0.1, L_5 = 0.1, W_e = 0.01, z = 0.4$.

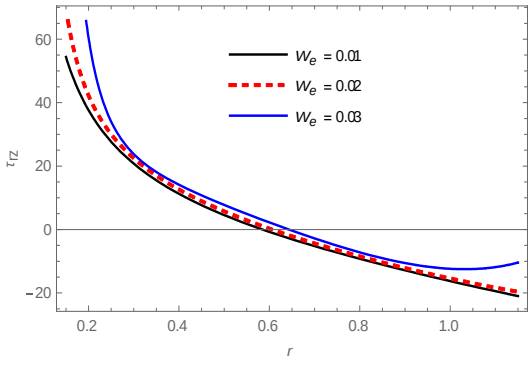

Figure 13 Shear-Stress for various values of W_e with $\varepsilon = 0.15, t = 0.1, L_1 = 0.1, L_2 = 0.5, L_3 = 0.1, L_4 = 0.1, L_5 = 0.1, \emptyset = 0.15, z = 0.4$.

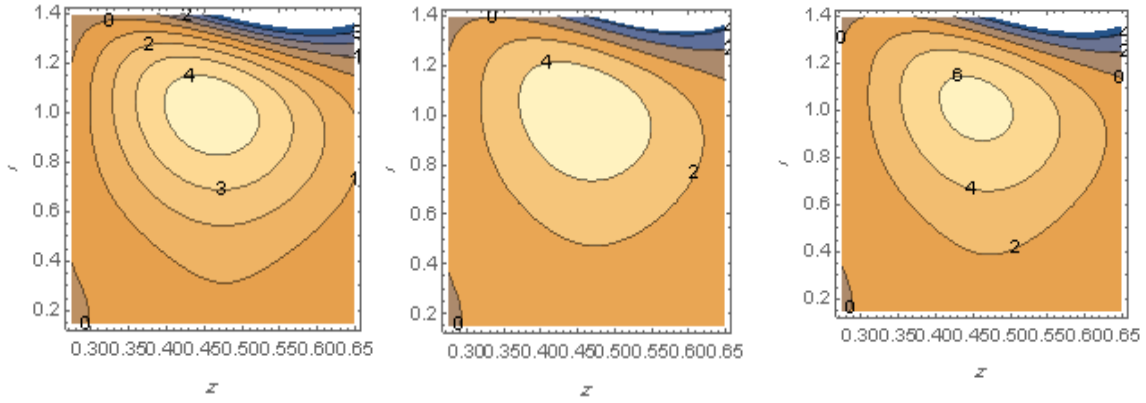

Figure 14: Wave frame streamlines for different values of $\phi = \{0.1,0.11,0.12\}$ at $\varepsilon = 0.12$, $W_e = 0.01$, $L_1 = 0.1$, $L_2 = 0.5$, $L_3 = 0.1$, $L_4 = 0.1$, $L_5 = 0.1$, $t = 0$.

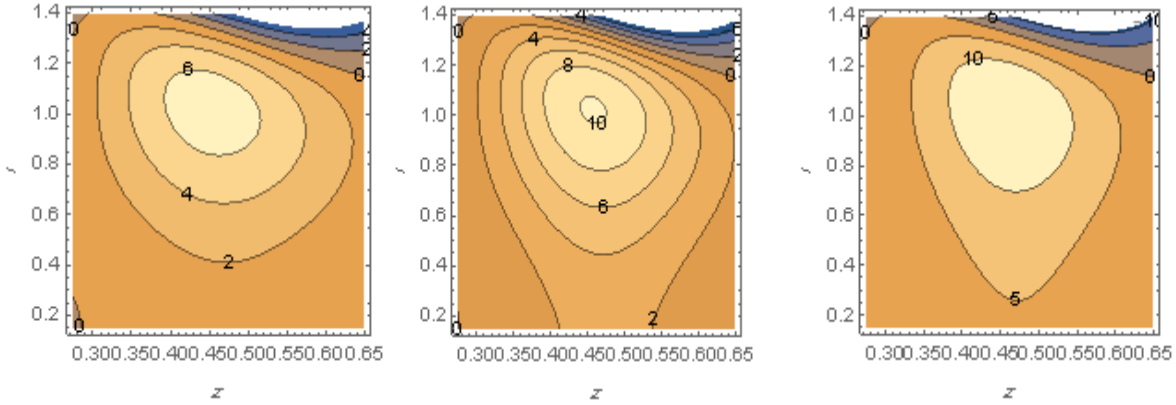

Figure 15: Wave frame streamlines for different values of $W_e = \{0.1,0.15,0.2\}$ at $\varepsilon = 0.12$, $\phi = 0.12$, $L_1 = 0.1$, $L_2 = 0.5$, $L_3 = 0.1$, $L_4 = 0.1$, $L_5 = 0.1$, $t = 0$.

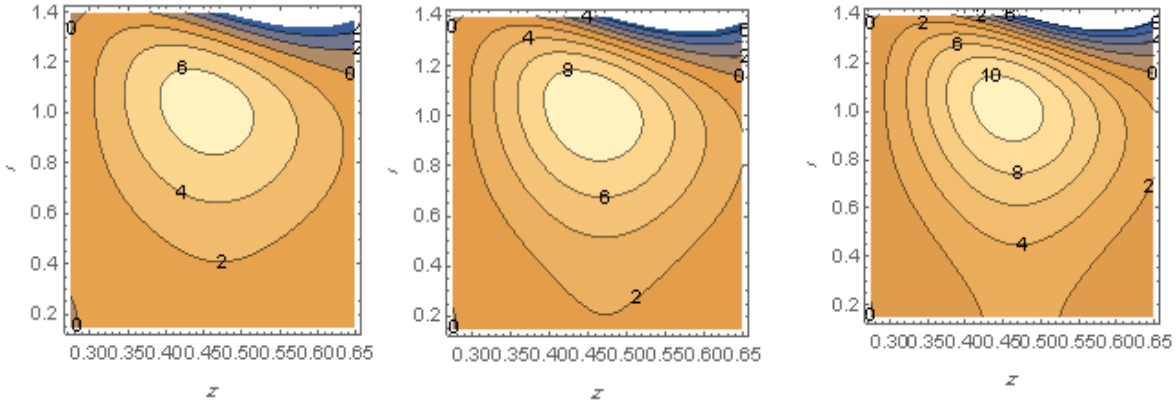

Figure 16: Wave frame streamlines for different values of $L_1 = \{0.1,0.11,0.12\}$ at $\varepsilon = 0.12$, $\phi = 0.12$, $W_e = 0.01$, $L_2 = 0.5$, $L_3 = 0.1$, $L_4 = 0.1$, $L_5 = 0.1$, $t = 0$.

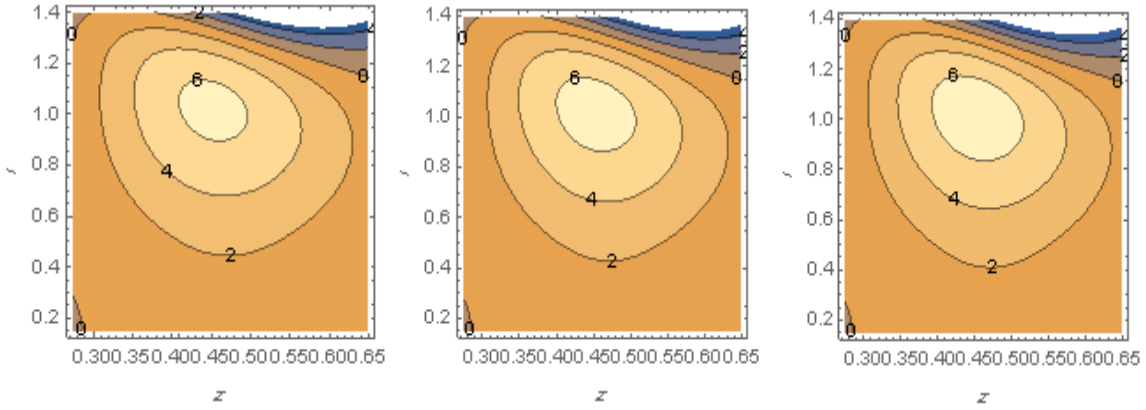

Figure 17: Wave frame streamlines for different values of $L_2 = \{0.3,0.4,0.5\}$ at $\varepsilon = 0.12$, $\phi = 0.12$, $W_e = 0.01$, $L_1 = 0.1$, $L_3 = 0.1$, $L_4 = 0.1$, $L_5 = 0.1$, t = 0.

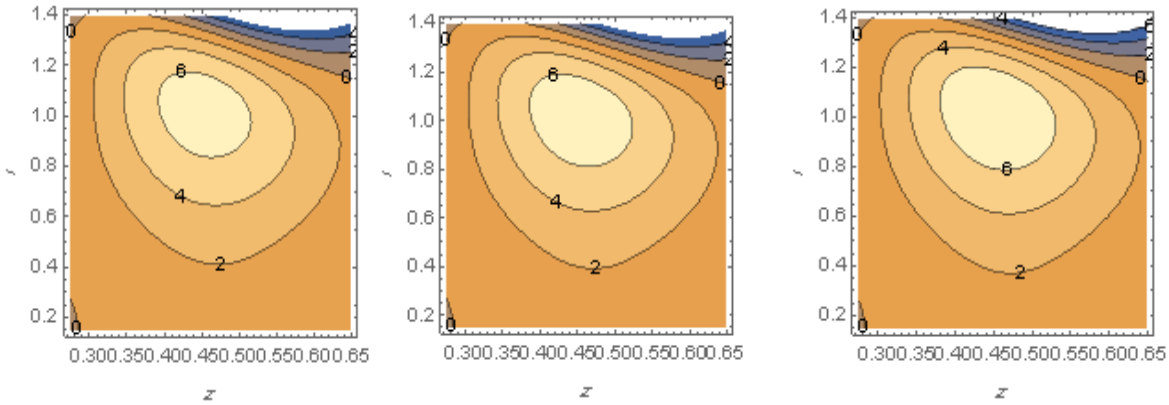

Figure 18: Wave frame streamlines for different values of $L_5 = \{0.1,1.1,2.1\}$ at $\varepsilon = 0.12$, $\phi = 0.12$, $W_e = 0.01$, $L_1 = 0.1$, $L_2 = 0.5$, $L_3 = 0.1$, $L_4 = 0.1$, t = 0.

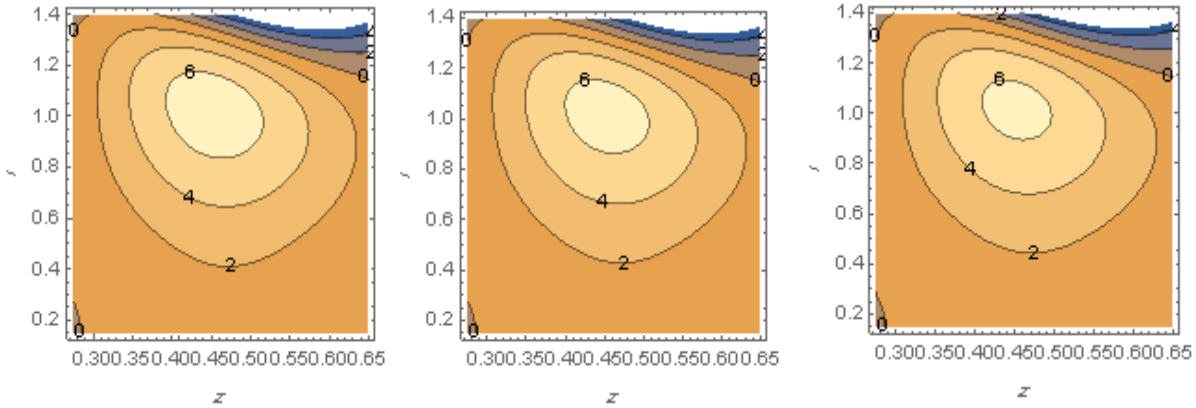

Figure 19: Wave frame streamlines for different values of $L_3 = \{0.1,0.2,0.3\}$ at $\varepsilon = 0.12$, $\phi = 0.12$, $W_e = 0.01$, $L_1 = 0.1$, $L_2 = 0.5$, $L_4 = 0.1$, $L_5 = 0.1$, t = 0.

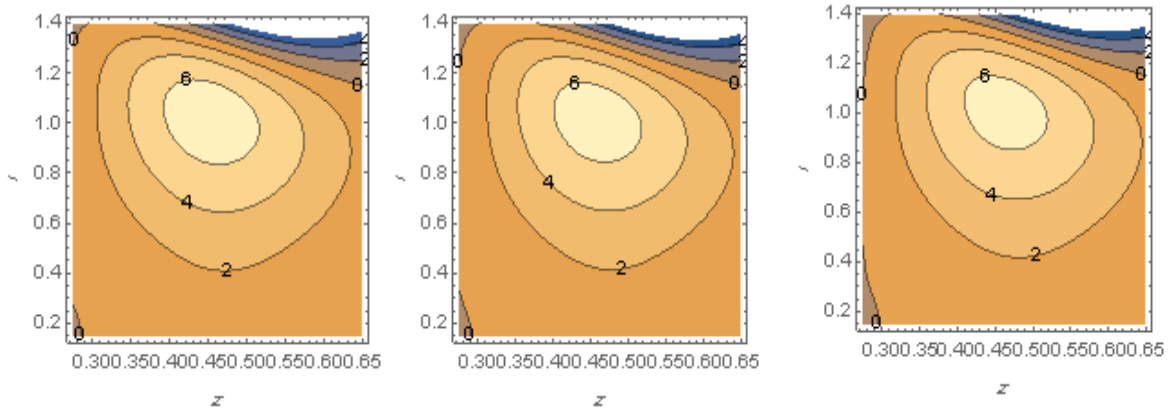

Figure 20: Wave frame streamlines for different values of $L_4 = \{0.1,1.1,2.1\}$ at $\varepsilon = 0.12$, $\phi = 0.12$, $W_e = 0.01$, $L_1 = 0.1$, $L_2 = 0.5$, $L_3 = 0.1$, $L_5 = 0.1$, t $= 0$.

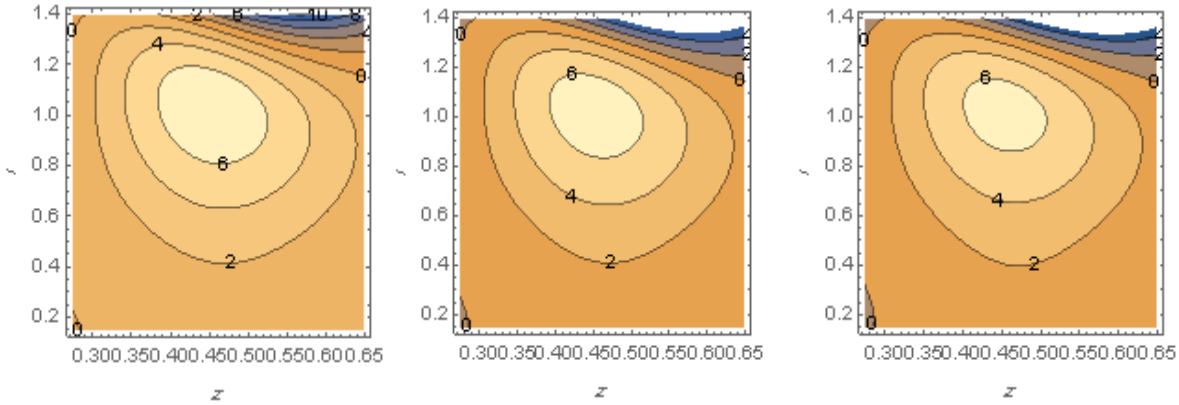

Figure 21: Wave frame streamlines for different values of $\varepsilon = \{0.1,0.12,0.14\}$ at $\phi = 0.12$, $W_e = 0.01$, $L_1 = 0.1$, $L_2 = 0.5$, $L_3 = 0.1$, $L_4 = 0.1$, $L_5 = 0.1$, t $= 0$.

9. Concluding Remarks

Significant results have been obtained by studying the effect of peristaltic flow of Williamson fluid through a channel of two overlapping tubes having the same center the inner is cylindrical solid and the outer is elastic rubber. Here are some results in brief :

- The effect Weissenberg number, outer wall, flexural stiffness of the wall, longitudinal tension per unit width and spring stiffness on fluid velocity direct, while the effect mass per unit area, coefficient of viscid damping, and inner wall are indirect.
- It was noted that the velocity curve is in the form of a parabola and that the greatest velocity of the fluid is in the center of the flow channel, while in the sides of the channel (the channel wall) the flow is the least.
- As for the shear stress, we note that its value fluctuates in the middle of the channel, where its amount at the solid wall is positive and is negative at the flexible wall. In addition, it is increasing at the solid wall and decreasing at the elastic wall when the increased outer wall, flexural stiffness of the wall, longitudinal tension per unit width, spring stiffness and vice versa for mass per unit area and coefficient of viscid damping, while the stress increases with the increase of inner wall and Weissenberg number.
- The trapped bolus increases and grows in the center of the channel and expands to the outer wall (elastic) with increasing outer wall, Weissenberg number, flexural stiffness, longitudinal tension per unit width, spring stiffness and vice versa for mass per unit area and coefficient of viscid damping the trapped bolus shrank.

References

[1] A. H. Hamid, T. Javed, B. Ahmed, and N. Ali, "Numerical study of two-dimensional non-Newtonian peristaltic flow for long wavelength and moderate Reynolds number," *J. Brazilian Soc. Mech. Sci. Eng.*, vol. 39, no. 11, pp. 4421–4430, 2017.

[2] A. Kavitha, R. H. Reddy, R. Saravana, and S. Sreenadh, "Peristaltic transport of a Jeffrey fluid in contact with a Newtonian fluid in an inclined channel," *Ain Shams Eng. J.*, vol. 8, no. 4, pp. 683–687, 2017.

[3] M. Gudekote and R. Choudhari, "Slip effects on peristaltic transport of Casson fluid in an inclined elastic tube with porous walls," *J. Adv. Res. Fluid Mech. Therm. Sci.*, vol. 43, no. 1, pp. 67–80, 2018.

[4] C. Rajashekhar, G. Manjunatha, K. V Prasad, B. B. Divya, and H. Vaidya, "Peristaltic transport of two-layered blood flow using Herschel–Bulkley Model," *Cogent Eng.*, vol. 5, no. 1, p. 1495592, 2018.

[5] T. Javed, B. Ahmed, A. H. Hamid, and M. Sajid, "Numerical analysis of peristaltic transport of Casson fluid for non-zero Reynolds number in presence of the magnetic field," *Nonlinear Eng.*, vol. 7, no. 3, pp. 183–193, 2018.

[6] B. Ahmed, T. Javed, and N. Ali, "Numerical study at moderate Reynolds number of peristaltic flow of micropolar fluid through a porous-saturated channel in magnetic field," *AIP Adv.*, vol. 8, no. 1, p. 15319, 2018.

[7] T. W. Latham, "Fluid motions in a peristaltic pump." Massachusetts Institute of Technology, 1966.

[8] A. H. Shapiro, "Pumping and retrograde diffusion in peristaltic waves," 1967.

[9] F. C. P. Yin and Y. C. Fung, "Comparison of theory and experiment in peristaltic transport," *J. Fluid Mech.*, vol. 47, no. 1, pp. 93–112, 1971.

[10] H. T. Tang and Y. C. Fung, "Fluid movement in a channel with permeable walls covered by porous media: A model of lung alveolar sheet," 1975.

[11] M. R. Salman and H. A. Ali, "Approximate Treatment for The MHD Peristaltic Transport of Jeffrey Fluid in Inclined Tapered Asymmetric Channel with Effects of Heat Transfer and Porous Medium," *Iraqi J. Sci.*, pp. 3342–3354, 2020.

[12] B. A. Almusawi and A. M. Abdulhadi, "Heat Transfer Analysis and Magnetohydrodynamics Effect on Peristaltic Transport of Ree–Eyring Fluid in Rotating Frame," *Iraqi J. Sci.*, vol. 62, no. 8, pp. 2714–2725, 2021.

[13] G. Dheia and S. Al-Khafajy, "Effects of wall properties and heat transfer on the peristaltic transport of a Jeffrey fluid through porous medium channel," *Math. theory Model.*, vol. 4, pp. 86–99, 2014.

[14] D. G. S. Al-Khafajy and A. M. Abdulhadi, "Effects of MHD and wall properties on the peristaltic transport of a Carreau fluid through porous medium," *J. J. Adv. Phys.*, vol. 6, no. 2, 2014.

[15] D. Al-Khafajy and A. M. Abdulhadi, "Influence of wall properties and heat transfer on the peristaltic transport of a Williamson fluid through porous medium channel," , *IJARSET, 2(11):970-981, 2015.*